Molecular Therapy
Nucleic Acids
Brief report

Antisense oligonucleotide targeting nicotinamide N-methyltransferase exhibits antitumor effects

Tomoaki Hara,[1] Sikun Meng,[1] Yuuya Kasahara,[2] Takashi Osawa,[3] Daisuke Motooka,[4] Hiromichi Sato,[1,5] Yasuko Arao,[1] Yoshiko Saito,[1] Kana Inoue,[1] Yumiko Hamano,[1] Yuichiro Doki,[5] Hidetoshi Eguchi,[5] Satoshi Obika,[3] and Hideshi Ishii[1]

[1]Department of Medical Data Science, Center of Medical Innovation and Translational Research, Osaka University Graduate School of Medicine, Osaka 565-0871, Japan; [2]National Institutes of Biomedical Innovation, Health and Nutrition, Osaka 567-0085, Japan; [3]Graduate School of Pharmaceutical Sciences, Osaka University, Osaka 565-0871, Japan; [4]Genome Information Research Center, Research Institute for Microbial Diseases, Osaka University, Osaka 565-0871, Japan; [5]Department of Gastroenterological Surgery, Osaka University Graduate School of Medicine, Osaka 565-0871, Japan

Nicotinamide N-methyltransferase (NNMT) is one of the methyltransferase family genes. It consumes S-adenosyl-l-methionine (SAM), which is required for DNA methylation and histone methylation for epigenetic regulation, to produce 1-methylnicotinamide from nicotinamide, a source of NAD^+, thus affecting energy metabolism and epigenetics. Recent studies have shown that *NNMT* is highly expressed in cancer tissues, mainly in the stroma, and worsens prognosis. Therefore, NNMT is attracting attention as a new target for cancer therapy. In this study, we generated 2′,4′-BNA/LNA-modified gapmer phosphorothioate antisense oligonucleotides that inhibit *NNMT* expression and examined their antitumor effects. The antisense oligonucleotide candidates were finally narrowed down to eight sequences, and when they were examined for their inhibitory effect on *NNMT* expression in cancer cells, all of the sequences showed inhibitory effects. The most effective one was conjugated with a small molecule compound that targets the stroma of cancer tissues. The antitumor effect was examined in a mouse model of cancer cell transplantation, and the antitumor effect was enhanced in the group treated with the antisense oligonucleotide. These results indicate that *NNMT* antisense oligonucleotide drugs targeting the stroma are promising as novel anticancer agents.

INTRODUCTION

Nicotinamide N-methyltransferase (NNMT) is a metabolic enzyme that uses S-adenosyl-l-methionine (SAM) to methylate nicotinamide to produce 1-methyl-nicotinamide (1-MNA).[1] Nicotinamide is absorbed from outside the body as niacin and is a raw material for NAD^+, which is important in energy metabolism.[2,3] Therefore, NNMT is involved in energy metabolism by regulating the supply of raw materials for NAD^+ synthesis. SAM is consumed for DNA methylation and histone methylation, which are necessary for epigenetic regulation.[4,5] Therefore, NNMT is also involved in epigenetic regulation by consuming SAM. NNMT has recently attracted attention as a target for anticancer agents.[6,7] 1-MNA generated by NNMT in cancer-associated fibroblasts (CAFs) is taken up by T cells, one of the immune cells, and induces T cell suppression through suppression of interferon gamma (IFN-γ) expression and tumor necrosis factor alpha (TNF-α) expression, thereby promoting cancer growth.[8] Proteomic analysis in ovarian cancer revealed CAF-specific expression of NNMT, and NNMT expression in CAF consumed SAMs and reduced histone methylation.[9] NNMT is highly expressed in breast cancer, and 1-MNA binds to ubiquitin-conjugating enzyme 12 (UBC12), enhancing neddylation-pathway-mediated p27 degradation by stabilizing UBC12, which is required for cullin-1 neddylation, and promotes cell-cycle progression.[10] In colorectal cancer, NNMT is expressed mainly in stroma, and its high expression in early stage cancers is associated with poor prognosis.[11] In liver cancer, high expression of NNMT in hepatic stellate cells (HSCs) can alter the methylation pattern of histone H3K27 and induce the generation of more stable splice variants of CD44, leading to hepatocellular carcinoma (HCC) invasion and metastasis.[12] Hedgehog signaling is activated in pancreatic cancer, and NNMT is one of its targets.[13] Thus, the expression of NNMT in cancer tissues plays an important role in cancer progression. In this study, we prepared 2′,4′-BNA/LNA-modified gapmer phosphorothioate (PS) antisense oligonucleotides (ASOs) as *NNMT* inhibitors and demonstrated that they function as novel inhibitors of NNMT.

Received 11 November 2024; accepted 25 April 2025;
https://doi.org/10.1016/j.omtn.2025.102548.

Correspondence: Satoshi Obika, Graduate School of Pharmaceutical Sciences, Osaka University, Osaka, Japan.
E-mail: obika@phs.osaka-u.ac.jp
Correspondence: Hideshi Ishii, Department of Medical Data Science, Center of Medical Innovation and Translational Research, Osaka University Graduate School of Medicine, Osaka, Japan.
E-mail: hishii@gesurg.med.osaka-u.ac.jp

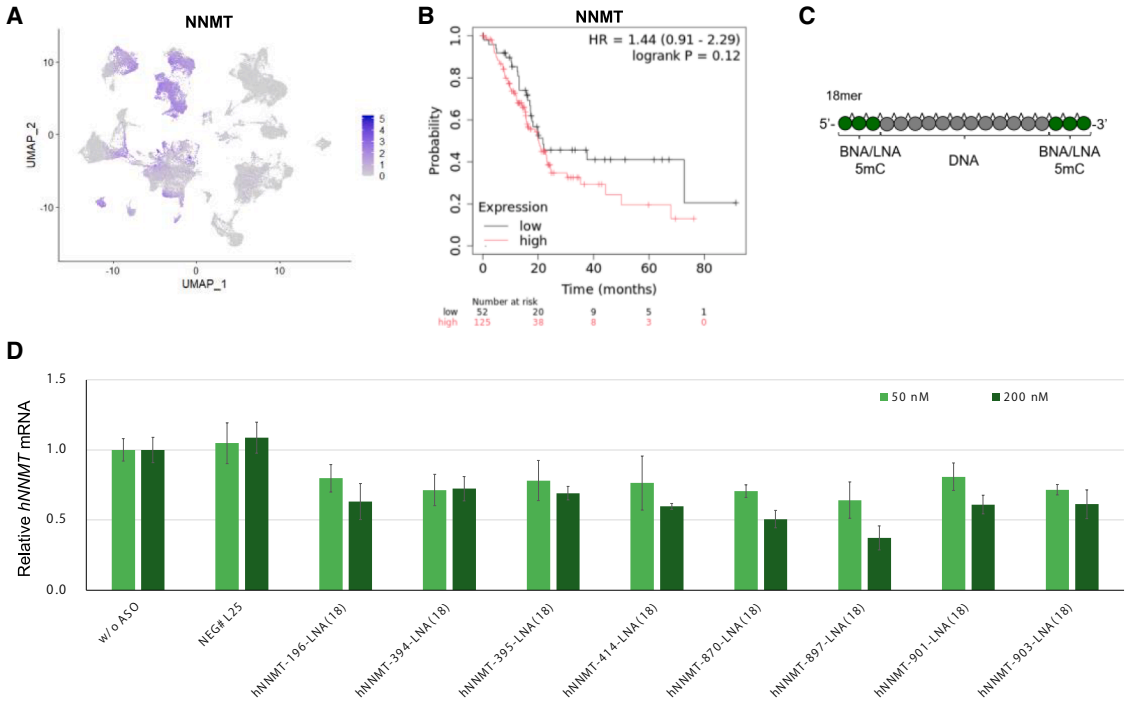

Figure 1. The design of ASO targeting *NNMT*

(A) *NNMT* expression in pancreatic cancer scRNA-seq data. (B) Kaplan-Meier curve of *NNMT*. Data for pancreatic ductal adenocarcinoma in Pan-cancer RNA-seq in the Kaplan-Meier plotter database were used. (C) Composition of 18-based ASO. (D) Inhibitory effect of each ASO on *NNMT* expression in HT29 cells. Data are presented as mean ± SD.

RESULTS

In our previous study, we integrated pancreatic cancer single-cell analysis data and generated a pancreatic cancer cell map consisting of approximately 134,000 cells.[14] We then used it to examine *NNMT* expression and found that *NNMT* is highly expressed in CAFs (Figure 1A). We used a Kaplan-Meier plotter to examine the prognostic value of *NNMT* expression and found that the prognosis of pancreatic cancer was worse in the group with high *NNMT* expression (Figure 1B). Therefore, we decided to pursue drug discovery targeting NNMT. NNMT is an intracellular protein that does not lend itself to antibody targeting. In this study, 18-mer gapmer ASOs targeting the NNMT-coding mRNA was selected as the drug discovery modality. All phosphodiester linkages of these gapmer ASOs were replaced by PS linkages, and three 2′,4′-BNA/LNA[15,16] modifications were introduced in the wing regions at both ends of the sequence (Figure 1C). Based on the intramolecular secondary structure predicted by RNAfold,[17] non-stem regions were extracted from all regions of the *NNMT* mRNA (NM_006169.3). Among the ASO sequences complementary to the extracted regions, we selected ASO sequences with an appropriate binding affinity to RNA predicted by GC%, and ASOs themselves are unlikely to form intramolecular stems or polymers. In addition, the GGGenome: https://gggenome.dbcls.jp/ and Database for Drug Development with Genome and RNA sequences (D3G): https://d3g.riken.jp/ were used to exclude ASO sequences, with large numbers of genes containing sequences with two or fewer insertions/deletions/mismatches. Finally, eight ASOs were selected (Table 1).

Table 1. Sequences of eight antisense oligonucleotides

ASO	Sequences
hNNMT-196-LNA(18)	5(L)^5(L)^5(L)^g^a^g^g^g^t^t^a^a^a ^a^t^G(L)^G(L)^5(L)
hNNMT-394-LNA(18)	5(L)^A(L)^G(L)^t^g^a^c^g^a^c^g^a ^t^c^t^5(L)^5(L)^T(L)
hNNMT-395-LNA(18)	T(L)^5(L)^A(L)^g^t^g^a^c^g^a^c^g ^a^t^c^T(L)^5(L)^5(L)
hNNMT-414-LNA(18)	5(L)^A(L)^G(L)^g^t^t^c^t^g^g^t^c ^t^g^a^G(L)^T(L)^A(L)
hNNMT-870-LNA(18)	A(L)^G(L)^A(L)^a^t^a^a^c^t^t^t^g ^c^g^a^G(L)^A(L)^T(L)
hNNMT-897-LNA(18)	A(L)^A(L)^G(L)^t^c^c^t^t^c^g^t^t^g ^t^t^G(L)^G(L)^5(L)
hNNMT-901-LNA(18)	A(L)^G(L)^A(L)^a^a^a^g^t^c^c^t^t^c ^g^t^T(L)^G(L)^T(L)
hNNMT-903-LNA(18)	G(L)^G(L)^A(L)^g^a^a^a^a^g^t^c^c ^t^t^c^G(L)^T(L)^T(L)

5 for 5mC, L for BNA/LNA, and lower case for DNA.

To examine the inhibitory effect of ASOs on *NNMT* expression, HT29 cells, a human colorectal adenocarcinoma cell line, were used to

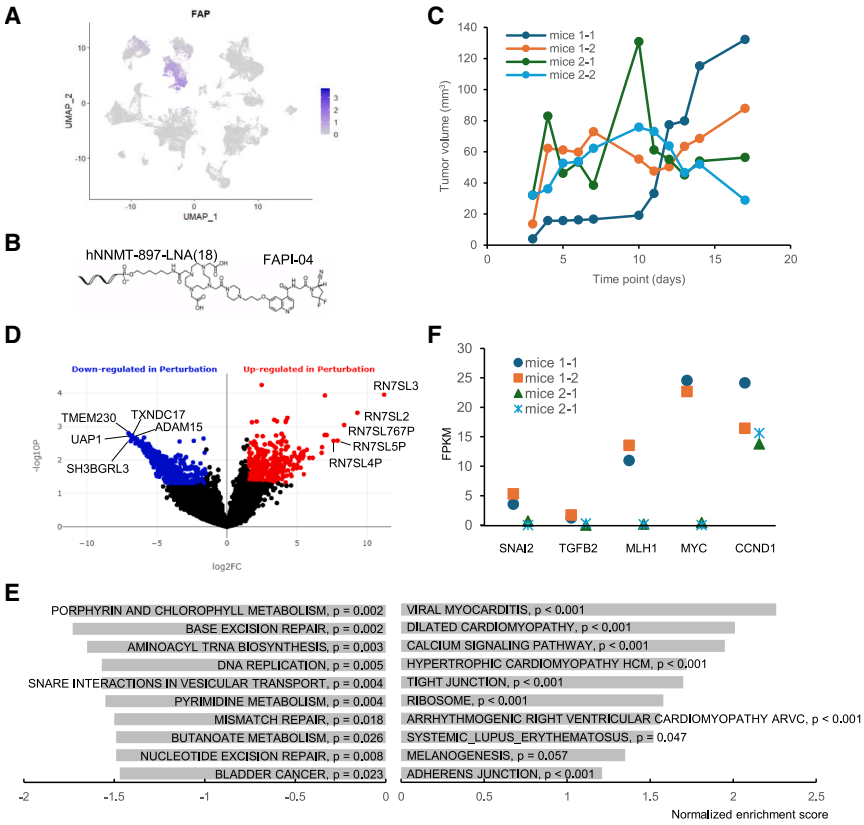

Figure 2. ASOs targeting *NNMT* exert antitumor effects

(A) Expression of *FAP* in pancreatic cancer scRNA-seq data. (B) Structure of FAP-binding small-molecule-conjugated ASO [hNNMT-897-LNA(18)]. FAPI-04 was used as FAP-binding compound. (C) Results of nucleic acid drug administration experiments using mouse xenograft models. Mice 1-1, 1-2 received 5-FU, PD-1 antibody, and CTLA4 antibody, mice 2-1, 2-2 received 5-FU, PD-1 antibody, and CTLA4 antibody, and ASOs were injected intravenously. (D) Volcano plot of genes with altered expression in cancer tissues resected after administration of ASO drugs in mouse xenograft models. Upregulated or downregulated genes in mice 2-1 and 2-2 compared to mice 1-1 and 1-2 by RNA-seq analysis were shown. (E) Gene set enrichment analysis (GSEA). Activated or inactivated signal pathway in mice 2-1 and 2-2 compared to mice 1-1 and 1-2 were shown. Statistical significance was determined using GSEA. Enrichment scores are shown with nominal *p*-values. (F) Gene expression levels for each gene obtained by RNA-seq. Values are fragments per kilobase of transcript per million mapped reads (FPKM).

evaluate *NNMT* expression by RT-qPCR. Compared to controls, mRNA expression levels were reduced by the eight ASOs. The expression level of *NNMT* was lower under the 200 nM ASO concentration condition than under the 50 nM condition, with hNNMT-897-LNA (18) showing the highest suppression (Figure 1D). Therefore, hNNMT-897-LNA(18) was selected as the final candidate sequence. To target CAF, we examined cell surface proteins of CAF using pancreatic cancer small conditional RNA sequencing (scRNA-seq) data and found that fibroblast activation protein (FAP) is specifically expressed in CAF (Figure 2A). Therefore, FAPI-04,[18] an FAP-binding compound, was conjugated to the ASO to add a function that specifically binds to and is taken up by CAFs (Figure 2B). This ASO was synthesized and purified by high-performance liquid chromatography (HPLC) (Figure S1). We decided to evaluate the efficacy of this final candidate in mouse xenograft models. MIA PaCa-2 cells, a human pancreatic cancer cell line, and 3T3 cells, mouse fibroblasts expressing FAP, were injected subcutaneously into mice, and the FAPI-04-conjugated ASO was injected intravenously. The antitumor effect was enhanced in the group treated with ASO in addition to 5-fluorouracil (5-FU), an anticancer drug, and immune checkpoint inhibitors (PD-1 antibody and CTLA4 antibody), compared to the group treated with 5-FU and immune checkpoint inhibitors alone (Figure 2C). To examine changes in gene expression in cancer cells induced by ASO administration, cancer tissue was excised from mice, RNA was extracted, and RNA-seq was performed to obtain gene expression data (Table S1). *RN7SL3*, *RN7SL2*, *RN7SL767P*, *RN7SL5P*, and *RN7SL4P* were detected as highly expressed genes and *TMEM230*, *UAP1*, *SH3BGRL3*, *TXNDC17*, and *ADAM15* as low-expressed genes (Figure 2D). Gene set enrichment analysis (GSEA) was performed to determine what signals were affected by ASO administration. The following data were obtained: viral myocarditis, dilated cardiomyopathy, calcium signaling pathway, hypertrophic cardiomyopathy, tight junction, ribosome, arrhythmogenic right ventricular cardiomyopathy, systemic_lupus_erythematosus, melanogenesis, and adherens junction were upregulated and porphyrin and chlorophyll metabolism, base excision repair, aminoacyl tRNA biosynthesis, DNA replication, SNARE interactions in vesicular transport, pyrimidine metabolism, mismatch repair, butanoate metabolism, nucleotide excision repair, and bladder cancer were downregulated (Figure 2E). In fact, the expression of cancer-related genes such as MYC, Cyclin D1 (CCND1), snail family transcriptional repressor 2 (SNAI2), transforming growth factor β 2 (TGF-β2), and MutL homolog 1 (MLH1), one of the DNA mismatch repair (MMR) genes, was downregulated in the FAPI-04-conjugated ASO-treated group (Figure 2F). We also examined the antitumor effect of FAPI-04-conjugated ASO in the A549 cell line derived from a non-small-cell lung carcinoma (NSCLC) and found a decrease in cell viability at 1,000 nM (Figure 3A). Comparison of the growth inhibitory effect of FAPI-04-conjugated ASO on A549 cells with an existing NNMT inhibitor, 6-methoxynicotinamide (JBSNF-00088),[19] showed that the effects were comparable (Figure 3B). In addition, a proliferation test using human lung-derived fibroblasts, MRC-5, showed that FAPI-04-conjugated ASO inhibited proliferation, and the effect was comparable to that of JBSNF-00088 (Figure 3C). When MRC-5 was cultured in medium containing FAPI-04-conjugated ASO or

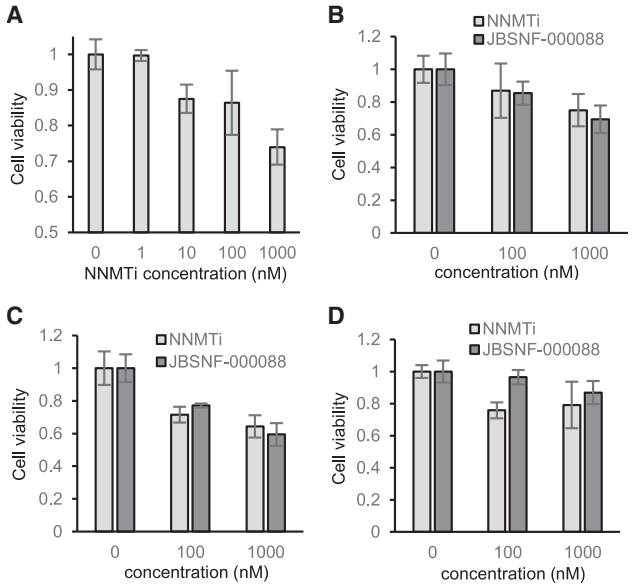

Figure 3. FAPI-04-conjugated ASO inhibits proliferation of A549 and MRC-5
(A) Cell viability in A549 cell line after 1 day of culture in each concentration of FAPI-04-conjugated ASO. (B) Cell viability in A549 after 2 days of culture in each concentration of FAPI-04-conjugated ASO or JBSNF-000088. (C) Cell viability in the MRC-5 cell line after 1 day of culture in each concentration of FAPI-04-conjugated ASO or JBSNF-000088. (D) Cell viability of A549 after culturing MRC-5 in each concentration of FAPI-04-conjugated ASO or JBSNF-000088 for 1 day and feeding the supernatant of the culture to A549 for 1 day. Data are presented as mean ± SD.

JBSNF-00088 and the supernatant of the culture was fed to A549 cells, growth inhibition was observed (Figure 3D). These results suggest that ASOs targeting NNMT have antitumor effects.

DISCUSSION

In this study, we aimed at drug discovery using ASOs targeting *NNMT*. NNMT is expressed mainly in CAFs in pancreatic cancer and has attracted much attention as a target because of its prognostic significance. Inhibition of *NNMT* expression by ASOs resulted in antitumor effects, indicating that *NNMT* is a target for drug discovery. We finally narrowed the number of ASOs to eight, and of the ASOs designed against *NNMT*, hNNMT-897-LNA(18) showed the highest *NNMT* inhibitory activity, suggesting that the suppressive effect varies depending on the mRNA target position. FAPI-04 is one of the small molecule compounds that bind strongly to FAP.[20] We therefore conjugated FAPI-04 to ASO to target FAP-expressing cells. The antitumor effect of FAPI-04-conjugated ASO was obtained in the xenograft mouse model, suggesting that a single modification of FAPI-04 is sufficient. The single modification of FAPI-04 may greatly contribute to the improvement of yield and ease of quality control in the drug synthesis process. NNMT has been reported to be involved in epigenetics.[21] In this study, we observed that MYC expression was downregulated by FAPI-04-conjugated ASO. MYC has been reported to be epigenetically regulated,[22] suggesting that FAPI-04-conjugated ASO affects epigenetic regulation through suppression of NNMT expression. In addition, SNAI2 and TGFB2 are involved in epithelial-mesenchymal transition (EMT),[23] suggesting that FAPI-04-conjugated ASO may inhibit metastasis by suppressing their expression. Although JBSNF-000088, an NNMT inhibitor, has been reported to have anti-tumor effects in NSCLC-derived PC9 cell line,[24] its cell viability at 1,000 nM was comparable to that of FAPI-04-conjugated ASO in this study using A549 cell line. Therefore, it is suggested that FAPI-04-conjugated ASO is applicable not only to pancreatic cancer but also to other types of cancer. Cancer cells in the ASO-treated group showed increased expression of *7SL* RNA family genes. *7SL* RNAs are RNAs that constitute signal recognition particles recognizing the translation of secreted proteins and membrane proteins to recruit them to the endoplasmic reticulum.[25] *7SL* RNA has been reported to activate immunity.[26] We have also shown that *7SL* RNAs may express micropeptide in oncogenic situations.[27] Therefore, ASO administration may have activated *7SL* RNA, resulting in an antitumor effect. Thus, ASO may be a promising anticancer agent by targeting *NNMT*.

MATERIALS AND METHODS

Gene expression analysis using scRNA-seq data

Our previously constructed database[14] was used to analyze *NNMT* and *FAP* expression in pancreatic cancer tissues. pk_all.rds file was loaded into R Seurat, and *NNMT* and *FAP* expression plot was shown by FeaturePlot.

The Kaplan-Meier curve for *NNMT*

The Kaplan-Meier curve was created from pancreatic ductal adenocarcinoma in Pan-cancer RNA-seq in the Kaplan-Meier plotter database.

RT-qPCR for cell-based NNMT inhibition experiments

HT29 (ATCC, Manassas, USA) was seeded in 96 well plates of 2,000 cells each and cultured in McCoy's 5a (Thermo Fisher SCIENTIFIC, Chino, USA) containing 10% fetal bovine serum (FBS) (Cosmo Bio Co., Ltd., Tokyo, Japan) for 1 day. Medium was replaced with DMEM low-glucose (Nacalai Tesque, Inc., Kyoto, Japan) containing 10% FBS, and ASOs were transfected by the Ca^{2+} enrichment of medium (CEM) method[28] and cultured for 1 day. Cells were collected, cDNA was prepared by SuperPrep Cell Lysis & RT Kit for qPCR (TOYOBO, Osaka, Japan), and RT-qPCR was performed by Power UP SYBR Green Master Mix for qPCR (Thermo Fisher SCIENTIFIC, Chino, USA). Conditions were as follows: preheating at 95°C for 20 s, denature at 95°C for 3 s, and extension at 60°C for 30 s. Denature and extension were repeated for 45 cycles. As internal standards, 200 nM each of *GAPDH* forward primer (5′-GAGTCA ACGGGATTTGGTCGT-3′) and *GAPDH* reverse primer (5′-GAC AAGCTTCCCGTTCTCAG-3′) were used. For *NNMT* quantification, 200 nM each of *NNMT* forward primer (5′-GCTGAAGAAAG AGAGCCAGAGAGG-3′) and *NNMT* reverse primer (5′-GAGTCA CATCACACTTCAGCAC-3′) were used. NEG#L25 (5′-AGACTCT GAACAAAA-3′) was used as ASO for negative control (underlined upper case for 2′,4′-BNA/LNA, upper case for DNA, all internucleotide linkages are PS). ASOs except for FAPI-04-conjugated one

and the primers for qPCR were purchased from GeneDesign, Inc., Ibaragi, Japan.

HPLC purification and MALDI-TOF mass characterization

SHIMADZU CBM-20A, DGU-20A_{5R}, LC-20AD, CTO-20A, SPD-20A, and FRC-10A (SHIMADZU, Kyoto, Japan) were utilized. The conjugation yield was calculated from peak values recorded at 260 nm wavelength on a microvolume UV-VIS spectrophotometer, DeNovix DS-11 (DeNovix, Wilmington, USA). MALDI-TOF mass spectra of an FAPI-04-conjugated ASO were recorded on a BRUKER Daltonics autoflex maX TOF/TOF mass spectrometer (BRUKER, Billerica, USA).

Animal experiments

Mouse experiments were performed after approval by the Osaka University Animal Experiments Committee. Mouse NIH/3T3 Tet-On 3G cell lines (Clontech, Mountain View, USA) were transfected with FAP expression plasmids, which were generated by incorporating the FAP gene synthesized artificially by GenScript between the Bam HI (NIPPON GENE, Tokyo, Japan) and Sal I (NIPPON GENE, Tokyo, Japan) sites of pTRE-Dual2 vector (Clontech, Mountain View, USA). A mixture of 5×10^6 MIA PaCa-2 cells (ATCC, Manassas, USA) and 2.5×10^6 FAP-expressing mouse 3T3 cells, 10% Corning Matrigel Growth Factor Reduced (GFR) Basement Membrane Matrix, LDEV-free (Corning Inc., Corning, USA), and doxycycline (1 μg/mL) in DMEM containing 10% FBS was injected subcutaneously into the back of mice as 250 μL cell solution. Mice were NOD/SCID mice (CLEA Japan, Inc., Tokyo, Japan). At 3, 5, 7, and 10 days after cell transplantation, 200 μg of 5-FU (10 mg/mL dissolved in PBS; FUJIFILM Wako Pure Chemical Corp., Osaka, Japan), 93.5 μg PD-1 antibody (Bio X Cell, Lebanon, USA), 90.6 μg CTLA4 antibody (Bio X Cell, Lebanon, USA), and the ASOs were injected intravenously. Tumors were measured with a caliper after transplantation, and tumor volume was calculated as: major axis × minor axis × minor axis × 0.5.

RNA-seq

Tumors excised from mouse were RNA-extracted with ISOGEN (NIPPON GENE, Tokyo, Japan), and RNA-seq was requested to the Genome Analysis Laboratory of the Research Institute for Microbial Diseases, Osaka University. Libraries were prepared with SMART-Seq HT Kit (Clontech, Mountain View, USA) and Nextera XT (Illumina, San Diego, USA), and RNA-seq was performed with NovaSeq6000 in 101 bp paired-end mode. The Rhelixa's RNA-seq pipeline (Rhelixa, Tokyo, Japan) of the Institute of Genetics was used from the resulting FASTQ files. The Rhelixa RNA-seq pipeline used FastQC for quality check, trimming with Trimmomatic, mapping with Hisat2, and gene expression with featureCounts. Volcano plots were drawn in BioJupies, a software to analyze data on the website: https://maayanlab.cloud/biojupies/analyze. GSEA (GSEAPreranked) was performed using the expression variable gene data obtained in BioJupies by using GSEA software: https://www.gsea-msigdb.org/gsea/index.jsp.

Cell proliferation assay

For the determination of viable cell counts of the A549 cell line (ATCC, Manassas, USA) and MRC-5 cell line (kindly provided by Dr. Murakumo), those cells were spread in 96-well cell culture plates (Corning Inc., Corning, USA) at 3,000 cells/well, and FAPI-04-conjugated ASO or JBSNF-00088 (MedChemExpress, Monmouth Junction, USA) was added to three wells per condition. PBS (Nacalai Tesque, Inc., Kyoto, Japan) was added in 0 nM condition. After 1 or 2 days, 10 μL of cell count Reagent SF (Nacalai Tesque, Inc., Kyoto, Japan) was added to each well, and absorbance at 450 nm was measured 1 h later. In Figure 3D, A549 was cultured for 1 day, then medium was exchanged with culture supernatant of MRC-5 cultured for 1 day in FAPI-04-conjugated ASO or JBSNF-00088, and cell viability was measured 1 day later.

DATA AVAILABILITY

All data are included in this paper.

ACKNOWLEDGMENTS

This work was supported in part by a Grant-in-Aid for Scientific Research from the Ministry of Education, Culture, Sports, Science and Technology (grant nos. 18KK0251, 19K22658, 20H00541, 21K19526, 22H03146, 22K19559, 23K19505, 23K18313, and 16H06279 [PAGS]). This research was supported by AMED under grant numbers JP17cm0106414, JP21lm0203007, and JP23ym0126809. We would like to express our sincere gratitude to Dr. Murakumo for kindly providing the MRC-5 cells used in this study. The authors are grateful to all the laboratory members. The authors thank the Research Institute for Microbial Diseases, Osaka University, for RNA-seq. Computations were partially performed on the NIG supercomputer at ROIS National Institute of Genetics.

AUTHOR CONTRIBUTIONS

T.H., S.M., Y.K., T.O., S.O., and H.I. designed research; T.H., S.M., Y.K., T.O., D.M., H. S., Y.A., Y.S., K.I., Y.H., and H.I. performed research; Y.K. and T.O synthesized ASOs; T. H., S.M., Y.K., T.O., D.M., and H.I. analyzed data; Y.D., H.E., S.O., and H.I. supervised the study; T.H., S.M., Y.K., T.O., D.M., and H.I. wrote the paper.

DECLARATION OF INTERESTS

T.H., S.M., H.S., Y.A., Y.S., K.I., Y.H., and H.I. received Partial institutional endowments from Hirotsu Bio Science Inc. (Tokyo, Japan), Kinshu-kai Medical Corporation (Osaka, Japan), Kyowa-kai Medical Corporation (Osaka, Japan), IDEA Consultants Inc. (Tokyo, Japan), and Unitech Co., Ltd (Chiba, Japan).

SUPPLEMENTAL INFORMATION

Supplemental information can be found online at https://doi.org/10.1016/j.omtn.2025.102548.

REFERENCES

1. Wang, W., Yang, C., Wang, T., and Deng, H. (2022). Complex roles of nicotinamide *N*-methyltransferase in cancer progression. Cell Death Dis. *13*, 267.
2. Campagna, R., and Vignini, A. (2023). NAD^+ Homeostasis and NAD^+-Consuming Enzymes: Implications for Vascular Health. Antioxidants *12*, 376.
3. Conlon, N., and Ford, D. (2022). A systems-approach to NAD^+ restoration. Biochem. Pharmacol. *198*, 114946.
4. Takeda, Y., Chijimatsu, R., Vecchione, A., Arai, T., Kitagawa, T., Ofusa, K., Yabumoto, M., Hirotsu, T., Eguchi, H., Doki, Y., and Ishii, H. (2021). Impact of One-Carbon Metabolism-Driving Epitranscriptome as a Therapeutic Target for Gastrointestinal Cancer. Int. J. Mol. Sci. *22*, 7278.
5. Espe, M., Adam, A.C., Saito, T., and Skjærven, K.H. (2023). Methionine: An Indispensable Amino Acid in Cellular Metabolism and Health of Atlantic Salmon. Aquac. Nutr. *2023*, 5706177.

6. Jabbari, P., Ardakany, M.R., Ebrahimi, S., and Rezaei, N. (2023). Nicotinamide N-methyl transferase and cancer-associated thrombosis: insights to prevention and management. Epigenomics *15*, 385–395.
7. Li, X.Y., Pi, Y.N., Chen, Y., Zhu, Q., and Xia, B.R. (2022). Nicotinamide N-Methyltransferase: A Promising Biomarker and Target for Human Cancer Therapy. Front. Oncol. *12*, 894744.
8. Kilgour, M.K., MacPherson, S., Zacharias, L.G., Ellis, A.E., Sheldon, R.D., Liu, E.Y., Keyes, S., Pauly, B., Carleton, G., Allard, B., et al. (2021). 1-Methylnicotinamide is an immune regulatory metabolite in human ovarian cancer. Sci. Adv. *7*, eabe1174.
9. Eckert, M.A., Coscia, F., Chryplewicz, A., Chang, J.W., Hernandez, K.M., Pan, S., Tienda, S.M., Nahotko, D.A., Li, G., Blaženović, I., et al. (2019). Proteomics reveals NNMT as a master metabolic regulator of cancer-associated fibroblasts. Nature *569*, 723–728.
10. Ma, Y., Huang, X., Wang, Y., Lei, Y., Yu, J., Yu, S., Gao, Y., Yang, J., Zhao, F., Yu, H., et al. (2024). NNMT/1-MNA Promote Cell-Cycle Progression of Breast Cancer by Targeting UBC12/Cullin-1-Mediated Degradation of P27 Proteins. Adv. Sci. *11*, e2305907.
11. Ogawa, M., Tanaka, A., Namba, K., Shia, J., Wang, J.Y., and Roehrl, M.H.A. (2022). Tumor stromal nicotinamide N-methyltransferase overexpression as a prognostic biomarker for poor clinical outcome in early-stage colorectal cancer. Sci. Rep. *12*, 2767.
12. Li, J., You, S., Zhang, S., Hu, Q., Wang, F., Chi, X., Zhao, W., Xie, C., Zhang, C., Yu, Y., et al. (2019). Elevated N-methyltransferase expression induced by hepatic stellate cells contributes to the metastasis of hepatocellular carcinoma via regulation of the CD44v3 isoform. Mol. Oncol. *13*, 1993–2009.
13. Feldmann, G., Habbe, N., Dhara, S., Bisht, S., Alvarez, H., Fendrich, V., Beaty, R., Mullendore, M., Karikari, C., Bardeesy, N., et al. (2008). Hedgehog inhibition prolongs survival in a genetically engineered mouse model of pancreatic cancer. Gut *57*, 1420–1430.
14. Chijimatsu, R.,, Kobayashi, S., Takeda, Y., Kitakaze, M., Tatekawa, S., Arao, Y., Nakayama, M., Tachibana, N., Saito, T., Ennishi, D., et al. (2022). Establishment of a reference single-cell RNA sequencing dataset for human pancreatic adenocarcinoma. iScience *25*, 104659.
15. Obika, S., Nanbu, D., Hari, Y., Morio, K.i., In, Y., Ishida, T., and Imanishi, T. (1997). Synthesis of 2′-*O*,4′-*C*-methyleneuridine and -cytidine. Novel bicyclic nucleosides having a fixed C_3, -endo sugar puckering. Tetrahedron Lett. *38*, 8735–8738.
16. Koshkin, A.A., Singh, S.K., Nielsen, P., Rajwanshi, V.K., Kumar, R., Meldgaard, M., Olsen, C.E., and Wengel, J. (1998). LNA (Locked Nucleic Acids): Synthesis of the adenine, cytosine, guanine, 5-methylcytosine, thymine and uracil bicyclonucleoside monomers, oligomerisation, and unprecedented nucleic acid recognition. Tetrahedron *54*, 3607–3630.
17. Gruber, A.R., Lorenz, R., Bernhart, S.H., Neuböck, R., and Hofacker, I.L. (2008). The Vienna RNA websuite. Nucleic Acids Res. *36*, W70–W74.
18. Lindner, T., Loktev, A., Altmann, A., Giesel, F., Kratochwil, C., Debus, J., Jäger, D., Mier, W., and Haberkorn, U. (2018). Development of Quinoline-Based Theranostic Ligands for the Targeting of Fibroblast Activation Protein. J. Nucl. Med. *59*, 1415–1422.
19. Kannt, A., Rajagopal, S., Kadnur, S.V., Suresh, J., Bhamidipati, R.K., Swaminathan, S., Hallur, M.S., Kristam, R., Elvert, R., Czech, J., et al. (2018). A small molecule inhibitor of Nicotinamide N-methyltransferase for the treatment of metabolic disorders. Sci. Rep. *8*, 3660.
20. Loktev, A., Lindner, T., Burger, E.M., Altmann, A., Giesel, F., Kratochwil, C., Debus, J., Marmé, F., Jäger, D., Mier, W., and Haberkorn, U. (2019). Development of Fibroblast Activation Protein-Targeted Radiotracers with Improved Tumor Retention. J. Nucl. Med. *60*, 1421–1429.
21. Ulanovskaya, O.A., Zuhl, A.M., and Cravatt, B.F. (2013). NNMT promotes epigenetic remodeling in cancer by creating a metabolic methylation sink. Nat. Chem. Biol. *9*, 300–306.
22. Fatma, H., Maurya, S.K., and Siddique, H.R. (2022). Epigenetic modifications of c-MYC: Role in cancer cell reprogramming, progression and chemoresistance. Semin. Cancer Biol. *83*, 166–176.
23. Aomatsu, K., Arao, T., Sugioka, K., Matsumoto, K., Tamura, D., Kudo, K., Kaneda, H., Tanaka, K., Fujita, Y., Shimomura, Y., and Nishio, K. (2011). TGF-β induces sustained upregulation of SNAI1 and SNAI2 through Smad and non-Smad pathways in a human corneal epithelial cell line. Investig. Ophthalmol. Vis. Sci. *52*, 2437–2443.
24. Wang, J., Liu, X., Huang, Y., Li, P., Yang, M., Zeng, S., Chen, D., Wang, Q., Liu, H., Luo, K., and Deng, J. (2022). Targeting nicotinamide N-methyltransferase overcomes resistance to EGFR-TKI in non-small cell lung cancer cells. Cell Death Discov. *8*, 170.
25. Kellogg, M.K., Miller, S.C., Tikhonova, E.B., and Karamyshev, A.L. (2021). SRPassing Co-translational Targeting: The Role of the Signal Recognition Particle in Protein Targeting and mRNA Protection. Int. J. Mol. Sci. *22*, 6284.
26. Johnson, L.R., Lee, D.Y., Eacret, J.S., Ye, D., June, C.H., and Minn, A.J. (2021). The immunostimulatory RNA RN7SL1 enables CAR-T cells to enhance autonomous and endogenous immune function. Cell *184*, 4981–4995.e14.
27. Hara, T., Meng, S., Tsuji, Y., Arao, Y., Saito, Y., Sato, H., Motooka, D., Uchida, S., and Ishii, H. (2024). RN7SL1 may be translated under oncogenic conditions. Proc. Natl. Acad. Sci. USA *121*, e2312322121.
28. Hori, S.I., Yamamoto, T., Waki, R., Wada, S., Wada, F., Noda, M., and Obika, S. (2015). Ca^{2+} enrichment in culture medium potentiates effect of oligonucleotides. Nucleic Acids Res. *43*, e128.